6.1 Introduction

As discussed in the previous chapters, the main disadvantage associated with magnesium based implants is their high corrosion rate and low mechanical strength. In this context present chapter focuses on efforts to prepare some new composites by addition of a new reinforcement 1393 BAG (bioactive glass) to the new alloy system having composition 3% aluminum, 2 % zinc and 0.6% calcium and rest magnesium. The present chapter describes the synthesis and characterization of Mg3Al2Zn0.6Ca.xBAG composites, where (x = 0, 10 and 15). The detailed method adopted for the preparation of the alloy and 1393 BAG (bioactive glass) has been explained in previous chapter (chapter 4, section 4.2). The nomenclature of the composites has been mentioned in Table 6.1.

Table 6.1: Nomenclature of the composites prepared

S.N	Base composition	1393 BAG (%)	Designation
1.	Mg3Al2Zn0.6Ca	0	Mg3Al2Zn0.6Ca
2.	Mg3Al2Zn0.6Ca	10	Mg3Al2Zn0.6Ca10BAG
3.	Mg3Al2Zn0.6Ca	15	Mg3Al2Zn0.6Ca15BAG

The composite specimens prepared were then characterized and their mechanical properties viz. hardness, young's modulus, flexural strength, and compressive strength were examined. To get the microstructural examination and surface characterization SEM

and XRD tests were performed. To know the degradation rate of the prepared composite in surrounding media, the corrosion tests were performed in SBF (detailed explanation in chapter 3 section). To estimate the amount of Mg^{+2} ions released in the SBF at different time intervals AAS tests were performed after 1, 3 and 7 days.

6.2 Results and Discussion

6.2.1 X-ray Diffraction (XRD)

The XRD of all the composite specimens after the sintering are shown in Fig. 6.1 and Fig. 6.2 respectively.

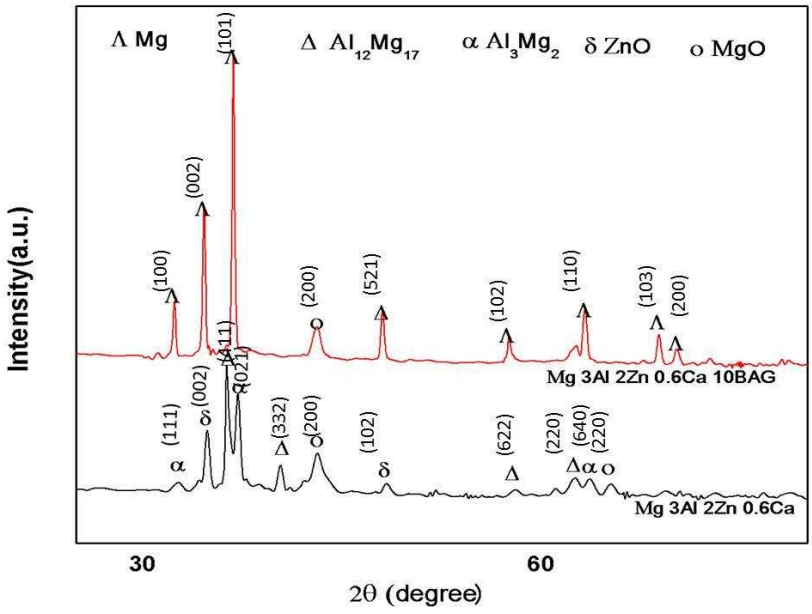

FIGURE 6.1: XRD pattern of Mg3Al2Zn0.6Ca & Mg3Al2Zn0.6Ca10BAG composites after sintering

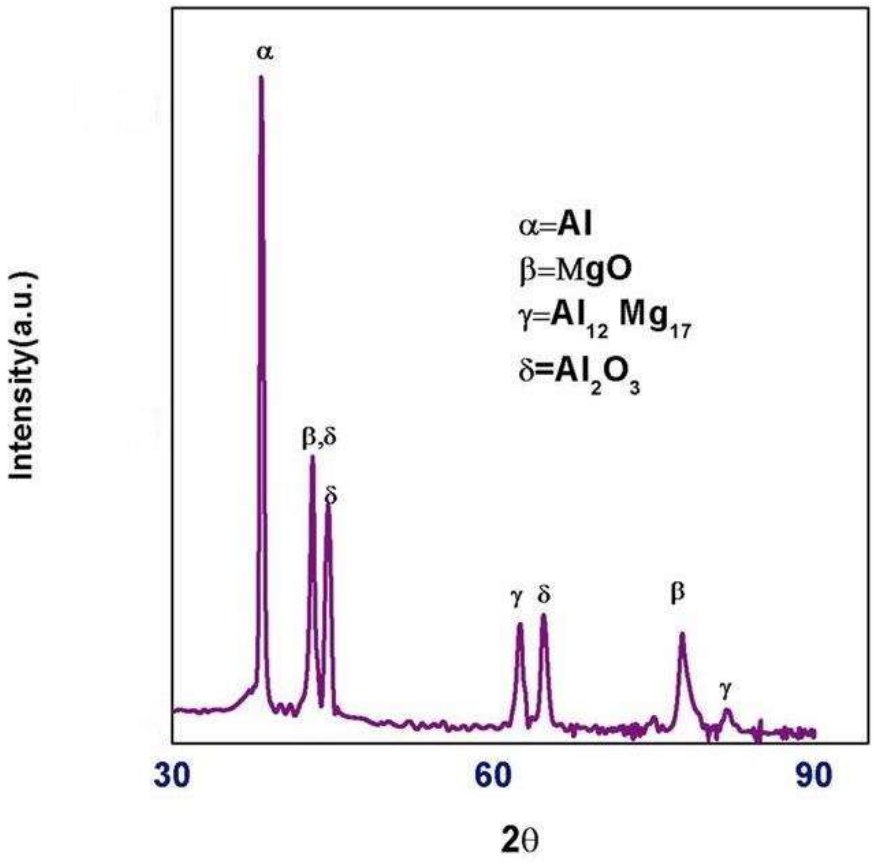

FIGURE 6.2: XRD pattern of Mg3Al2Zn0.6Ca15BAG composite after sintering

Fig. 6.1 reveals the XRD peaks of composites after sintering, the phases present were predominantly complex intermetallic compounds like $Al_{12}Mg_{17}$. Calcium present in the composite controls the oxidation of magnesium and supports the proper sintering of the composites. In both the base alloy, as well as that added with 10% 1393 BAG and 15 % BAG, the formation of $Al_{12}Mg_{17}$ and Al_3Mg_2 phase was formed which causes to improvement in the mechanical properties. Some peaks of oxides of zinc and magnesium have also been formed along with metallic phases of magnesium.

6.2.2 Microstructure Evolution

The microstructure of the composites after sintering (before immersion tests) is shown in Fig. 6.3. The SEM images of the sintered alloy shows uniform surfaces with no differentiating structure on the surface. The sintered alloy consists of inter metallic phases and elemental Mg and Al mainly as it is evident from the EDS analysis as shown in Fig. 6.4. The sintered alloy was expected to have shown the presence of MgO but it presences was very small and not detected considerably, which is desirable and it suggests the better sintering of the samples.

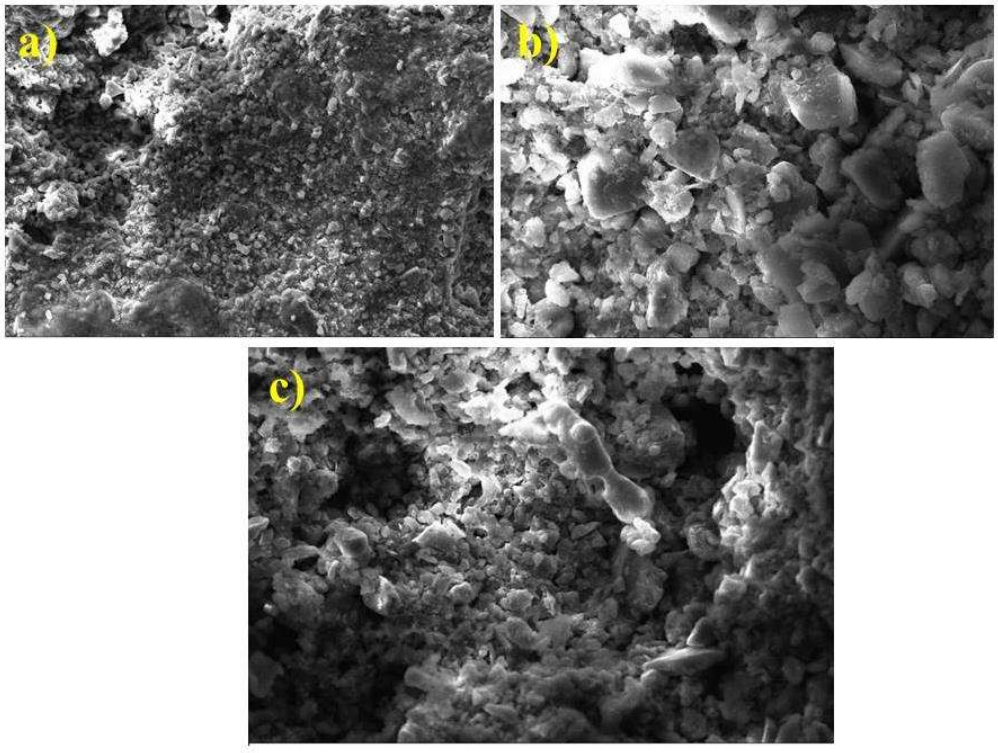

FIGURE 6.3: SEM images of samples after sintering (before immersion test) (a) Mg3Al2Zn0.6Ca, (b) Mg3Al2Zn0.6Ca10BAG, (c) Mg3Al2Zn0.6Ca15BAG

After immersion in SBF for different days, all the composites have shown development of HA layers on the surfaces. This HA layer is more formed in the samples containing more 1393 BAG. The development of HA layer as immersion time have the same nature in all the composites. Figure 6.4 shows SEM and EDS images of sample with 0 1393BAG and 10 1393BAG.

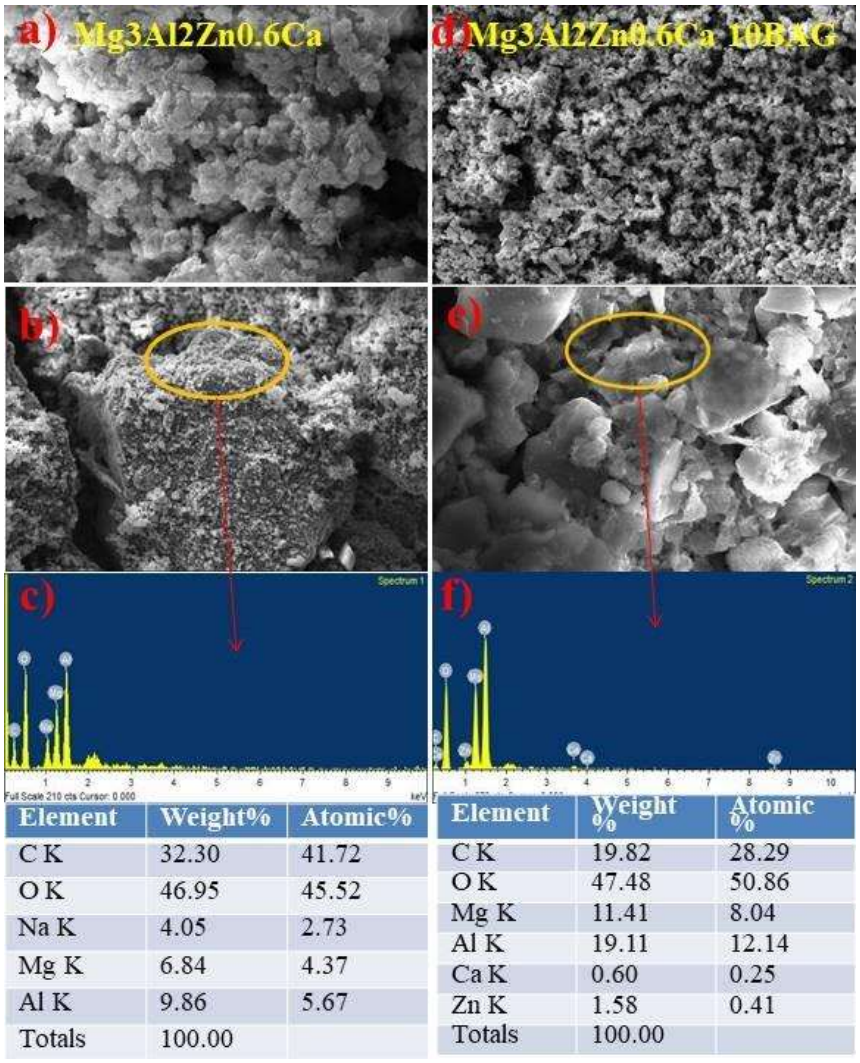

Element	Weight%	Atomic%
C K	32.30	41.72
O K	46.95	45.52
Na K	4.05	2.73
Mg K	6.84	4.37
Al K	9.86	5.67
Totals	100.00	

Element	Weight %	Atomic %
C K	19.82	28.29
O K	47.48	50.86
Mg K	11.41	8.04
Al K	19.11	12.14
Ca K	0.60	0.25
Zn K	1.58	0.41
Totals	100.00	

FIGURE 6.4: SEM & EDS images of composites Mg3Al2Zn0.6Ca a) 7 days b) 14 days c)EDS analysis and Mg3Al2Zn0.6Ca10BAG d) 7 days e) 14 days f) EDS analysis

The development of HA layers from 1st day onwards is shown in the figures 6.5 to 6.9 along with EDS data for the composite Mg3Al2Zn0.6Ca15BAG.

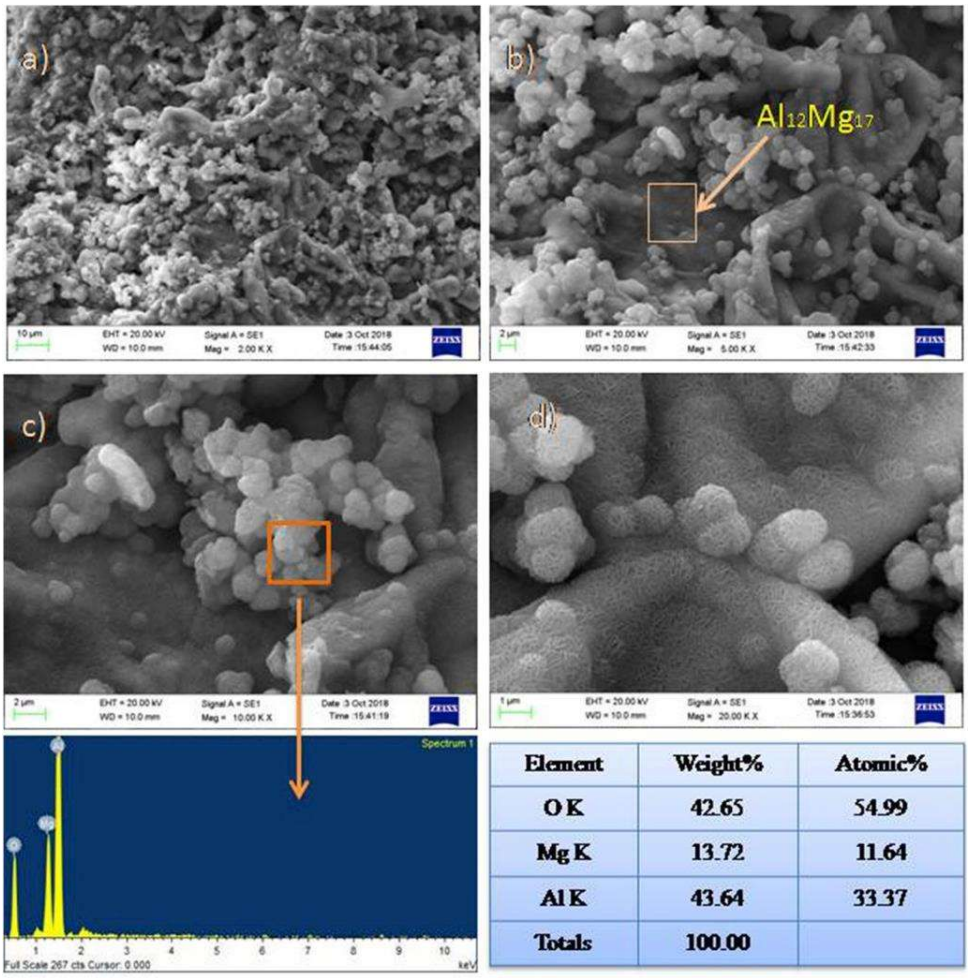

Element	Weight%	Atomic%
O K	42.65	54.99
Mg K	13.72	11.64
Al K	43.64	33.37
Totals	100.00	

FIGURE 6.5. SEM with EDX images of Mg3Al2Zn0.6Ca15BAG composite after immersion in SBF for 1 days at magnification (a) 2000X, (b)5000X, (c)10000X, (d)20000X

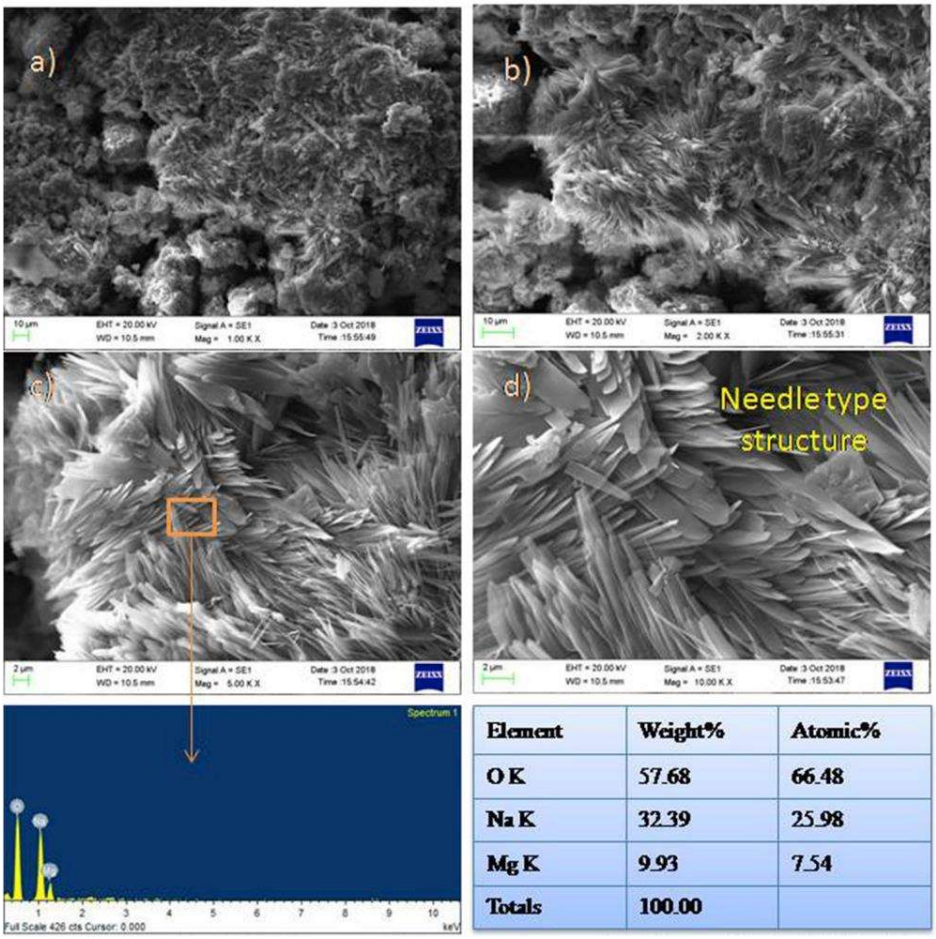

Element	Weight%	Atomic%
O K	57.68	66.48
Na K	32.39	25.98
Mg K	9.93	7.54
Totals	100.00	

FIGURE 6.6: SEM with EDX images of Mg3Al2Zn0.6Ca15BAG composite after immersion in SBF for 3 days at magnification (a) 1000X, (b) 2000X, (c) 5000X, (d)10000X

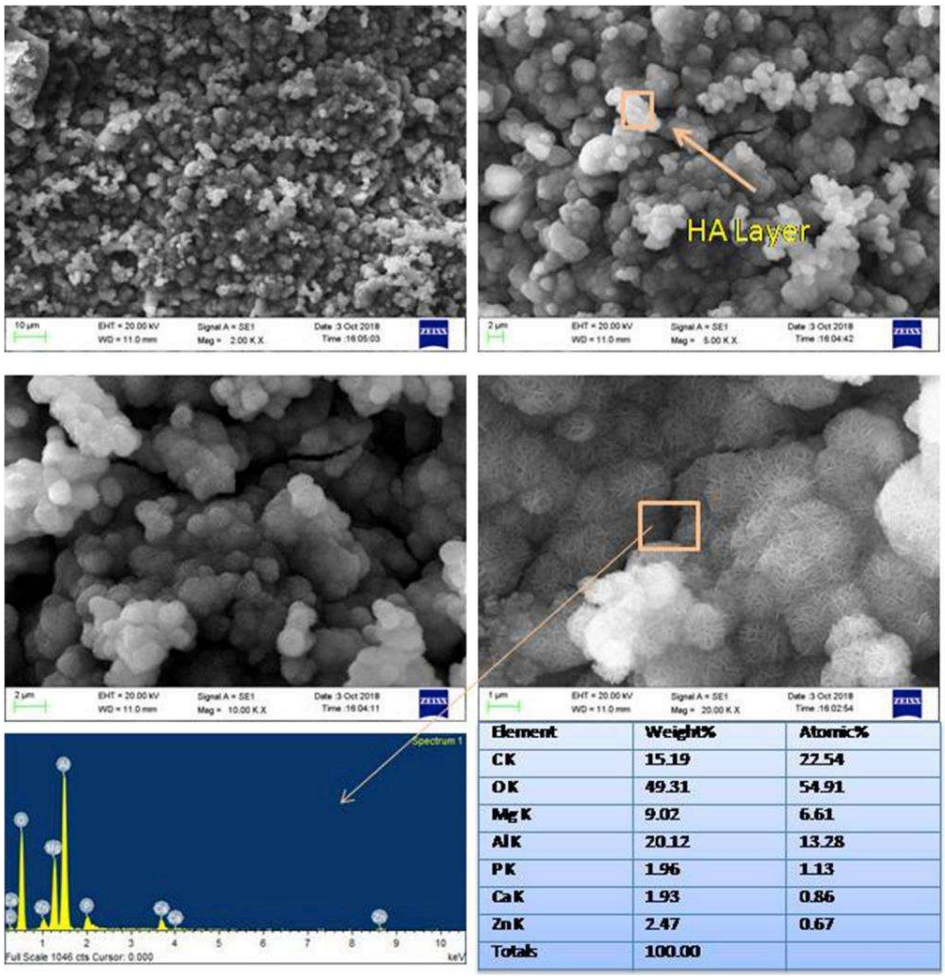

Element	Weight%	Atomic%
CK	15.19	22.54
OK	49.31	54.91
MgK	9.02	6.61
AlK	20.12	13.28
PK	1.96	1.13
CaK	1.93	0.86
ZnK	2.47	0.67
Totals	100.00	

FIGURE 6.7: SEM and EDX images of Mg3Al2Zn0.6Ca15BAG composite after immersion in SBF for 5 days at magnification (a) 2000X, (b) 5000X, (c) 10000X, (d) 20000X.

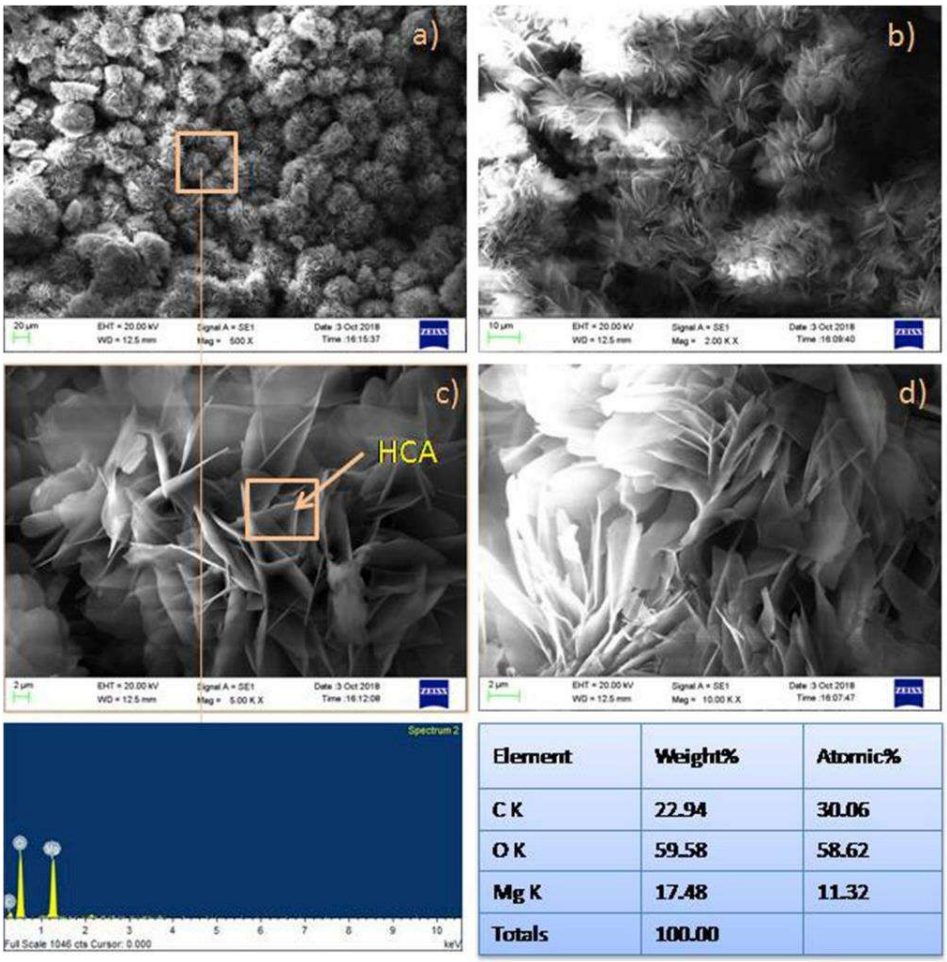

Element	Weight%	Atomic%
C K	22.94	30.06
O K	59.58	58.62
Mg K	17.48	11.32
Totals	100.00	

FIGURE 6.8: SEM and EDX images of Mg3Al2Zn0.6Ca15BAG composite after immersion in SBF for 7 days at magnification (a) 500X, (b) 2000X, (c) 5000X, (d) 10000X

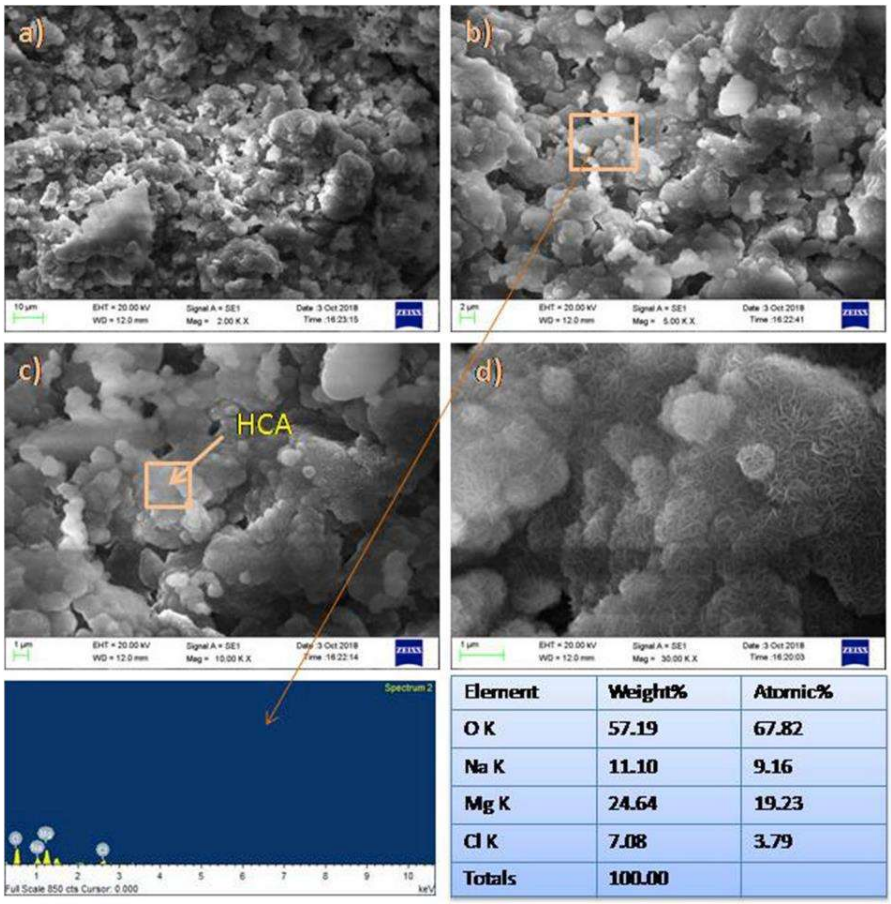

Element	Weight%	Atomic%
O K	57.19	67.82
Na K	11.10	9.16
Mg K	24.64	19.23
Cl K	7.08	3.79
Totals	100.00	

FIGURE 6.9 SEM and EDX images of Mg3Al2Zn0.6Ca15BAG composite after immersion in SBF for 14 days at magnification (a) 2000X, (b)5000X, (c)10000X, (d)30000X

The surface characteristics of the composite prepared were also analyzed with the XRD data of the corroded surface. Figure 6.10 shows the XRD results of the composite Mg3Al2Zn0.6Ca15BAG after different immersion time.

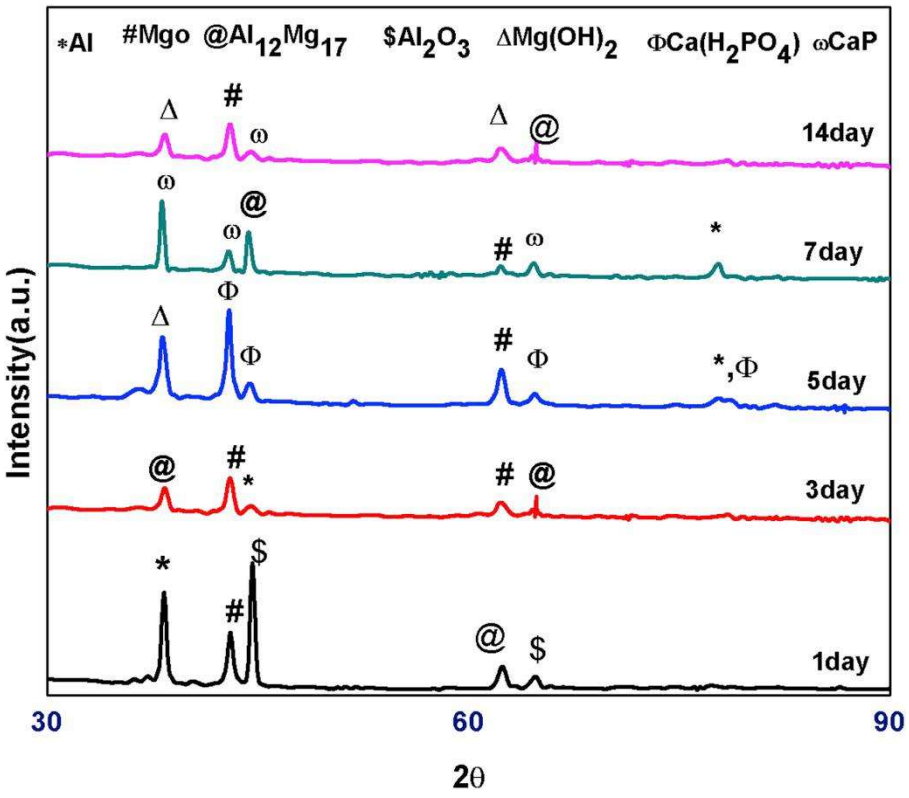

FIGURE 6.10: XRD pattern of Mg3Al2Zn0.6Ca15BAG composite after 1,3,5,7 and 14 days of immersion in SBF

After being dipped in the SBF, the XRD pattern of test samples after immersion for 1, 3, 5, 7 and 14 days, has been shown in Fig. 6.10. The XRD data shows that after 1 day immersion in SBF, the formation of MgO and $Mg(OH)_2$ are in trace amount. Also the peaks of AlMg and some intermetallic compounds as $Al_{12}Mg_{17}$, $AlMg_2$ have been formed. After 3 days the intensity of MgO and $Mg(OH)_2$ has increased which are the reasons for decrease in corrosion rate. Fig. 6.10 shows the XRD patterns of the samples after immersion in SBF for 7 days and the results obtained shows the formation of crystalline phases after being dipped in SBF. Crystalline phase of hydroxyapatite $[Ca_{10}(PO_4)_6(OH)_2]$ and the diffraction peaks were formed which can be seen on SEM images of the surfaces

after the 7 days of immersion. Also the formation of Hydroxyapatite layer after the increase in immersion time helps to control the degradation rate. The corrosion rate in SBF further decreases after 7 days and nearly uniform results were obtained from 7 to 14 days.

6.2.3 Physical and mechanical characteristics

6.2.3.1 Total Porosity and Densification

The extent of proper sintering and strengthening of the composite depends normally on the porosity and densification. The porosity and densification of the samples are mentioned in Table 6.2.

TABLE 6.2: Total porosity and densification of different composites

S.N	Sample	Densification (%)	Total Porosity (%)
1.	Mg3Al2Zn0.6Ca	85.88	14.12
2.	Mg3Al2Zn0.6Ca10BAG	88.13	11.87
3.	Mg3Al2Zn0.6Ca15BAG	87.99	12.01

The densification achieved for the different compositions were found to be maximum in the case of the sample Mg3Al2Zn0.6Ca10BAG. The homogeneity of distribution of reinforcement in composites normally depends on the ratio of matrix and reinforcement. Initially upto 10% addition densification in the composites were observed to increase but

at higher percentage, the densification was observed to decrease as in case of 15% 1393 BAG, this decrease in densification and increase in porosity was more dominant when the amount of reinforcement were further increased (say 20 %). This may happen because of the agglomeration and clustering of the bio- glass particles. Furthermore, the weak bonding between bio-glass and magnesium matrix interface creates gap in the microstructure leading to higher porosity value.

6.2.3.2 Mechanical characteristics

The average mechanical properties of the composite prepared are tabulated in Table 6.3

TABLE 6.3: Mechanical properties of different composites

S.N	Sample	Hardness (HV)	Young's Modulus (GPa)	Flexural Strength (MPa)	Compressive Strength (MPa)
1.	Mg3Al2Zn0.6Ca	118.7 ± 2.65	38.96 ± 3.12	115.23 ± 2.16	138.18 ± 3.12
2.	Mg3Al2Zn0.6Ca10BAG	124.4 ± 1.81	46.69 ± 2.27	128.89 ±2.14	149.11 ± 2.03
3.	Mg3Al2Zn0.6Ca15BAG	122 ± 1.16	50.9 ± 2.10	125.61 ± 1.67	146.46 ± 1.17

The mechanical strength of the composites greatly depends upon the extent of densification, proper sintering and minimum pores present in the composites. The results for mechanical properties show that the properties of composites with 10% and 15 % 1393 BAG have sufficient mechanical strength. The literature suggests that the reinforcement of hard particles to the matrix of a composite/ alloy affects the strengthening mechanism

of the matrix. The mechanical strength provided in present case can be attributed to the fact that the reinforced particles hinder the dislocations movement and provide strength to the matrix (B. Bobic, et al. 2014). Also, the mechanical strength depends on the grain size and pores in the specimen. This is the reason why at higher concentration of the reinforcement porosity increases due to agglomeration of particles. The mechanical characteristics shows that for the higher concentration of 1393 BAG, the strength will deteriorate, which is mainly due to improper densification, porosity effect and agglomeration of the reinforcement phase. In fact, for the composite with 1393 BAG percentage more that 15 %, due to the effect of porosity it deteriorates after 7 days of immersion in the corrosive media.

6.2.4 Electrochemical behavior

To evaluate the corrosion rate of anodized samples, potentio-dynamic tests were done to know the surface behavior. Electrochemical techniques are based on detection of corrosion of a metal by observing the effect of charge transfer process to a controlled electrochemical phenomenon. The potentio dynamic test gives the information about polarization curve from which the values of Corrosion potential (E_{corr}) and Current density (I_{corr}) of the samples can be interpreted (H.J. Flitt and D.P. Schweinsberg, 2005). The polarization curve is generated by potentiodynamic test as shown in Fig. 6.11 to 6.13. This was fitted by Ec-lab to provide the results of corrosion potential (Ecorr) and current density (Icorr) which helps in obtaining the data for corrosion rate (H.J. Flitt and D.P. Schweinsberg, 2005; Q. Zhao, 2013).

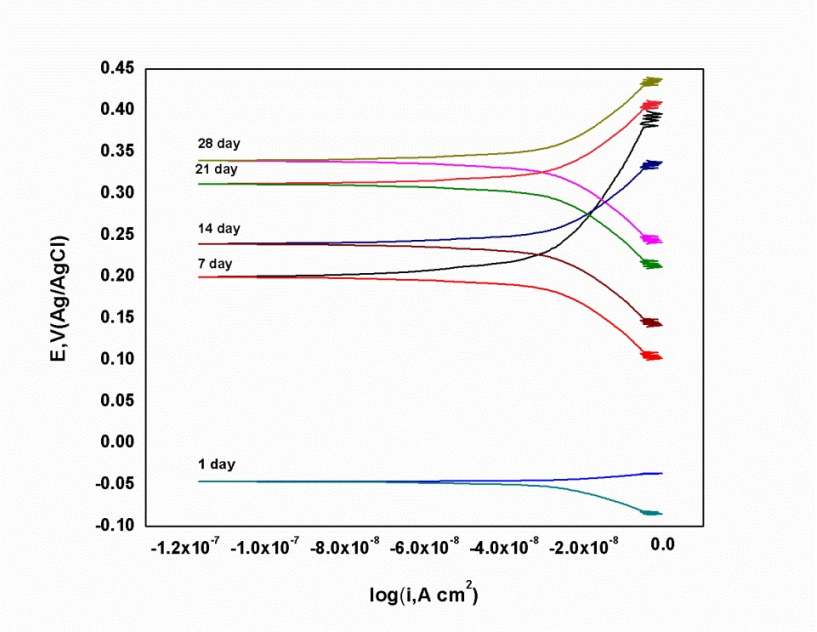

FIGURE 6.11: Potentiodynamic polarization curves of Mg3Al2Zn0.6Ca alloy after immersion in SBF solution

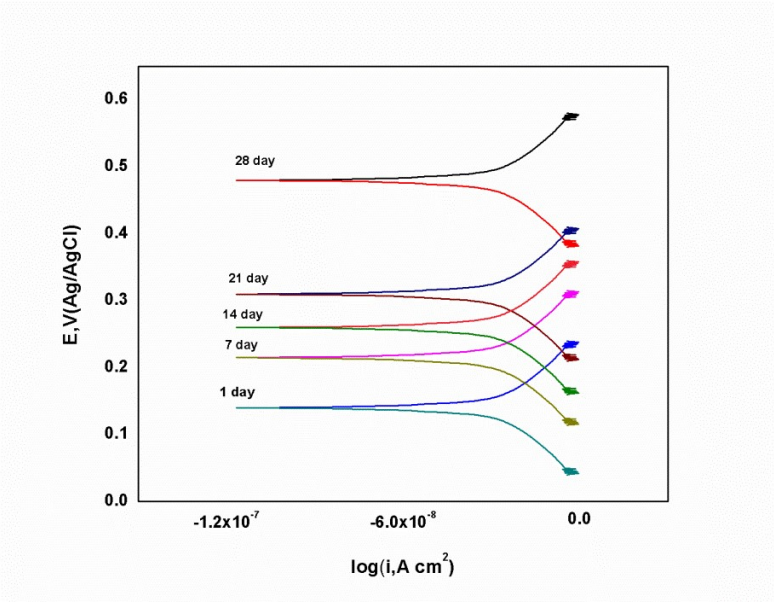

FIGURE 6.12: Potentiodynamic polarization curves of Mg3Al2Zn0.6Ca10BAG composite after immersion in SBF solution

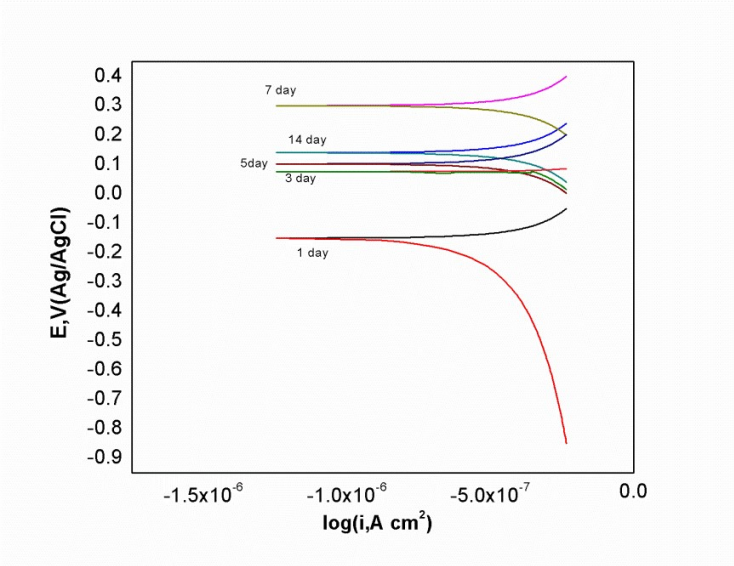

FIGURE 6.13: Potentiodynamic polarization curves of Mg3Al2Zn0.6Ca15 BAG composite after immersion in SBF solution

The values of Ecorr and Icorr of the samples has been evaluated and mentioned in Table 6.4 to Table 6.6. The corrosion rates interpreted from the polarization curve are mentioned in Fig. 6.6. & 6.7

TABLE 6.4: Corrosion potential, current density and corrosion rate of Mg3Al2Zn0.6Ca in potentiodynamic test

S.N.	Days	E_{corr} (mV)	I_{corr} ($\mu A/cm^2$)	Corrosion Rate (mmpy)
1.	1	-45.639	0.059	0.841
2.	7	205.828	0.057	0.247
3.	14	241.23	0.052	0.218
4.	21	313.230	0.052	0.034
5.	28	338.906	0.052	0.028

TABLE 6.5: Corrosion potential, current density and corrosion rate of Mg3Al2Zn0.6Ca10BAG in potentiodynamic test

S.N.	Days	E_{corr} (mV)	I_{corr} ($\mu A/cm^2$)	Corrosion Rate (mmpy)
1.	1	141.23	0.103	0.058
2.	7	178.88	0.038	0.049
3.	14	261.094	0.103	0.028
4.	21	317.176	0.092	0.022
5.	28	323.317	0.040	0.005

TABLE 6.6: Corrosion potential, current density and corrosion rate of Mg3Al2Zn0.6Ca15 BAG in potentiodynamic test

S.N.	Days	E_{corr} (mV)	I_{corr} ($\mu A/cm^2$)	Corrosion Rate (mmpy)
1.	1	-144.396	0.151	191.785
2.	3	196.390	0.0017	0.325
3.	5	229.075	0.00025	0.4102
4.	7	371.60	.00036	0.4572
5.	14	223.12	.000061	0.0850

The corrosion rate of all the specimens are presented in graphical form in Fig. 6.14 & 6.15

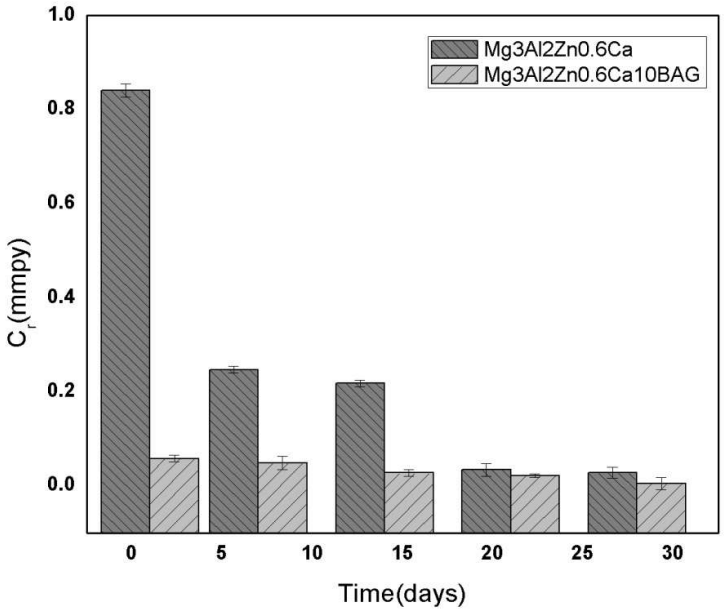

FIGURE 6.14: Variation of corrosion rate of Mg3Al2Zn0.6Ca & Mg3Al2Zn0.6Ca10BAG after immersion for different durations in SBF solution

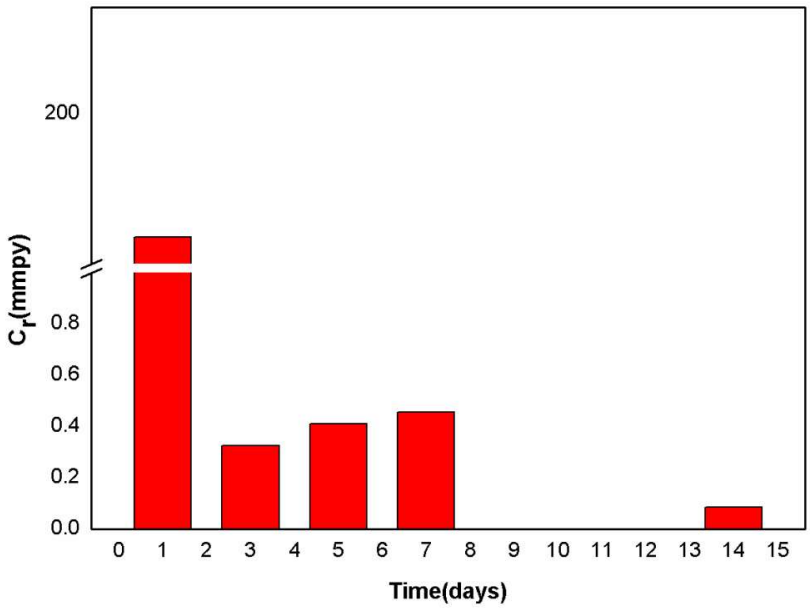

FIGURE 6.15: Variation of corrosion rate of Mg3Al2Zn0.6Ca15BAG after immersion for different durations in SBF solution

In the present case, the outcome obtained reveals that the corrosion rate was initially higher in all the cases i.e. for the composite with 0 % 1393 BAG as well as that added with 10% 1393 BAG and 15% 1393BAG. After 1 day, the corrosion potential value obtained for Mg3Al2Zn0.6Ca was obtained as -45.639 millivolt and the current density was 0.059 microamperes per cm^2. The value of the corrosion rate interpreted from the Tafel curve after 1 day, was 0.841 millimeters per year. For the composite added with 10% 1393 BAG, the corrosion potential value was obtained as 141.23 millivolts and the current density was 0.103 micro Ampere per cm^2, the corrosion rate evaluated was 0.058 mm per year. The corrosion potential of all the compositions were observed to increase with immersion time and the current density decreases with immersion time. The degradation of the magnesium-based alloy takes place as per the following equation (Y. Wang, et al. 2009).

$$Mg + H^+ + H_2O \rightarrow Mg^{2+} + OH^- + H_2 \qquad (6.1)$$

The corrosion products formed after immersion in SBF were mainly Magnesium Oxide or Magnesium Hydroxide. Also, the formation of phosphates, carbonates and hydroxyapatite takes place due to deposition of ions from SBF, which are earlier discussed and confirmed by SEM micrographs and corresponding EDX results (Y. Wang, et al. 2009). The addition of 1393 BAG in the base alloy Mg3Al2Zn0.6Ca promotes the HA layer development and it controls the degradation rate. The results acquired from SEM EDX and XRD shows the emergence of the above protective layers on the surface of composites. Corrosion rate of composite reinforced with 10 % 1393BAG was observed to be slower than that without 1393BAG because 1393 BAG being a bioactive material promotes the faster formation of HA layers (H. Tripathi, et al. 2019). In case of the composite added with 15 % 1393 BAG

the corrosion rate was again observed to be very high compared to that with 0% 1393 BAG and 10% 1393 BAG. After 1 day immersion of the sample in SBF, the corrosion potential value obtained was found to be -144.396 millivolt and the corresponding current density was 0.151 micro amperes per cm^2. After 1 day the value of corrosion rate obtained was 191.785 millimeter per year. After 3 days the corrosion potential increased drastically and became positive 196.390 mV and the current density decreased to 0.0017mm/year, also the corrosion rate decreased to 0.325 mm/year. It was observed that the corrosion potential and the current density have inverse relation i.e. the increase in corrosion potential leads to decrease in current density (H.J. Flitt and D.P. Schweinsberg, 2005). The negative value of corrosion potential indicates that the material is prone to corrosion and the more positive value shows that the material has achieved the nobility or in other words it will be less prone to corrosion. The initial higher corrosion rate is due to the high reactivity of magnesium, but as time passes the development of layers of HA and other products on the surface hinder the further corrosion of the composites. In fact, increase in the amount of 1393 BAG promotes development of protective layers of HA, but in case of composite with 15% 1393 BAG higher corrosion rate than that of 10 1393 BAG were observed, it is due to as discussed in previous section 6.2.3.1, the effect of porosity and densification comes into role and increases the corrosion rate of the samples. Corrosion being a very complex phenomena depends on lots of factors (H.J. Flitt and D.P. Schweinsberg, 2005), and in present case, the effect of densification, which in turn controls the mechanical properties and the development of corrosion layers have two intervening effects on corrosion. Also, the strengthening of the composites provided by the inclusion of 1393 BAG particles are mainly due to densification of the composites.

This densification and bonding of the molecules is due to grain size reduction and more grain boundaries act as more barriers against preferred crystallographic pitting, which reduces the corrosion rate of the composites (Y. Wang, 2009). Also the strengthening of the composite was due to the concept that the when the matrix is reinforced by some hard particle, it prevents the dislocation motions by creating obstacles at the grain boundary and hence increase the strength and corrosion characteristics of a composite material (J.A. Floro, et al. 1994).

6.2.5 Ion release estimation

The degradation of Mg^{+2} ions in the SBF were further analyzed by atom absorption spectroscopy (AAS) tests, which given the ionic concentration of Mg^{+2} in parts per million. From AAS results interpreted from Fig. 6.16, the initial concentration of Magnesium ions (Mg^{+2}) in SBF, for Mg3Al2Zn0.6Ca was found to be 10.642 ppm and it reached up to 11.092 ppm after 28 days. For Mg3Al2Zn0.6Ca10 BAG the release of Magnesium ions was having the same pattern, initially, the ions released were 10.4154 ppm, but comparatively lower concentration than base composition. Also, from Fig. 6.17, it was observed that the composite Mg3Al2Zn0.6Ca15 BAG released Mg^{+2} ions and the initial number of ions of magnesium in parts per million was 10.5268 and reached up toss 12.5452 ppm after 14 days, which had increased continuously, it shows that the dissolution of Mg^{+2} ions in the SBF was a continuous process at ionic level. The trend observed in ionic dissolution can be attributed to a strong bonding and reduced grain size as explained earlier. It has been observed that magnesium has a significant effect on osteoblastic cell differentiation. The release of magnesium around the implant promotes bone formation and it accelerates bone healing (A. Chaya, et al. 2015). The AAS results

shows that the results of corrosion tests and that of mechanical strength and densification were in agreement with each other and all have the same nature and this nature is well supported by estimation of ion release of magnesium.

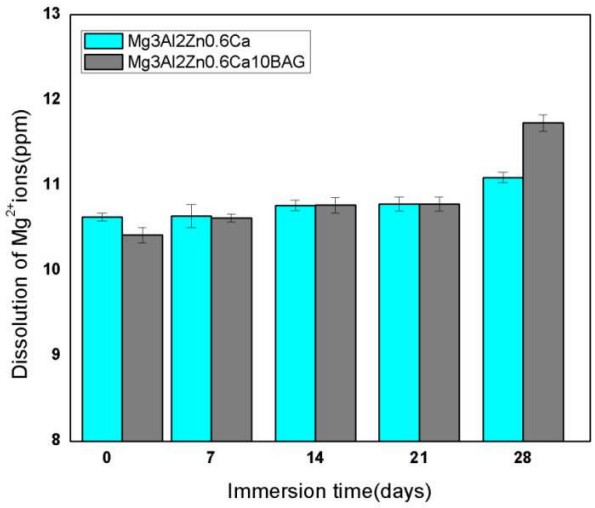

FIGURE 6.16 Release of Magnesium ions with immersion time for Mg3Al2Zn0.6Ca & Mg3Al2Zn0.6Ca10BAG composite

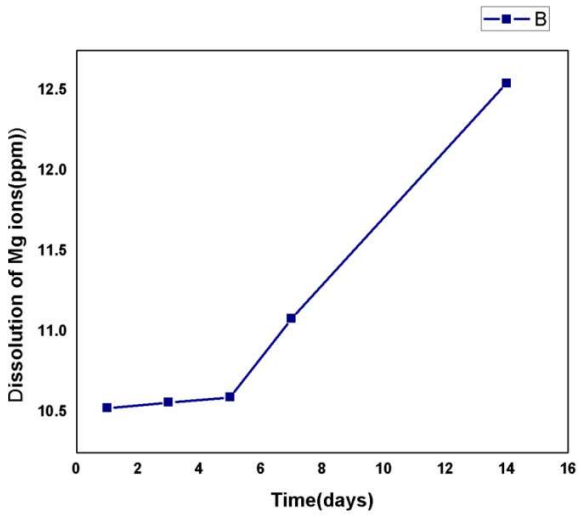

FIGURE 6.17 Release of Magnesium ions with immersion time for Mg3Al2Zn0.6Ca15BAG composite

6.3 Summary of the chapter

The present chapter is focused on the study of physical, mechanical, corrosion and ion release estimation of the newly developed composite by addition of 1393 BAG in different proportions. The chapter studied and characterized the corrosion products formed on the composite surface after immersion in corrosive media. The concluding remarks of work done are as follows:

1. It can be concluded that among all the composites added with 1393 BAG, the composite Mg3Al2Zn0.6Ca10BAG have optimized mechanical strength and corrosion resistance. The strength of the composites was observed to increase by the dispersion hardening mechanism and densification. At higher concentration of 1393 BAG, the properties deteriorate mainly due to porosity effect and less densification. Hence for the magnesium alloy Mg3Al2Zn0.6Ca when added with 10% 1393 BAG have maximum mechanical properties, above which the composite loses its strength.

2. The corrosion studies has revealed that the corrosion rate of the composite specimen were very high on the first day of immersion in the SBF, but as the time duration increased the formation of protective layers of $Mg(OH)_2$ and hydroxyapatite $[Ca_{10}(PO_4)_6(OH)_2]$ act as an agent to control the degradation and hence maintain mechanical integrity of the composites prepared. The study of corrosion surfaces were confirmed by both SEM and XRD data. It has also been found that with the increase in BAG content in the matrix, the corrosion rate were comparatively higher than the composite without BAG particle reinforcement, but at higher concentration the integrity of the composite was compromised and corrosion rate increased at higher concentration.

3. The AAS experiments suggest that the metal ions dissolve in the range of 10.642 ppm to

12.5452 ppm, which is well below the daily limit for human bodies i.e. 100 mg to 300 mg per day). It has been observed that magnesium has a significant effect on osteoblastic cell differentiation. The release of magnesium around the implant promotes bone formation and it accelerates bone healing.

4. This result opens the scope of application of the composite Mg3Al2Zn0.6Ca10BAG developed, as a potential implant, subjected to further working on its in vivo testing.